



---

# INVESTIGATION OF MICROSTRUCTURAL CHANGES USING: SCANNING ELECTRON MICROSCOPY, X-RAY DIFFRACTION, AND FOURIER TRANSFORM INFRARED SPECTROSCOPY

*Ansh Dagdi<sup>1</sup>, Kumarpal Singh<sup>2</sup>*

<sup>1</sup>Aryabhata College of Engineering and Research Center Ajmer, Rajasthan

<sup>2</sup>Aryabhata College of Engineering and Research Center Ajmer, Rajasthan

---

## ABSTRACT :

This study presents a comprehensive investigation into the microstructural changes of composite materials using advanced characterization techniques—Scanning Electron Microscopy (SEM), X-Ray Diffraction (XRD), and Fourier Transform Infrared Spectroscopy (FTIR). SEM analysis was employed to examine surface morphology and particle distribution at various treatment stages, revealing insights into pore structure, agglomeration, and fracture behavior. XRD provided critical information on crystalline phases and changes in crystallinity, enabling the identification of phase transformations due to thermal or chemical treatment.

FTIR spectroscopy was utilized to detect functional groups and bonding characteristics, highlighting chemical modifications in silicate and alumina-based matrices. The combined use of these techniques offers a multi-dimensional understanding of the physical and chemical evolution within the material, aiding in the correlation between microstructure and performance. The findings contribute to the optimization of composite material design for enhanced durability and functionality.

---

**Keywords:** Microstructural Analysis, Scanning Electron Microscopy (SEM), X-Ray Diffraction (XRD), Fourier Transform Infrared Spectroscopy (FTIR), Composite Materials, Crystalline Phase Analysis, Surface Morphology, Functional Groups, Material Characterization, Phase Transformation.

---

## INTRODUCTION

Understanding the microstructural behavior of materials is critical for predicting and enhancing their mechanical, thermal, and chemical performance. Microstructural changes often govern the long-term durability, strength, and functional characteristics of materials under various environmental or operational conditions. To accurately assess these changes, advanced analytical techniques are required that provide both morphological and chemical insights at the microscopic and atomic levels [1].

Scanning Electron Microscopy (SEM), X-Ray Diffraction (XRD), and Fourier Transform Infrared Spectroscopy (FTIR) are widely utilized tools in material science for microstructural and phase characterization. SEM offers high-resolution imaging of surface topography and particle morphology, revealing changes such as crack formation, pore distribution, and material densification. XRD is an essential technique for identifying crystalline phases and detecting phase transformations resulting from thermal or mechanical processing. Meanwhile, FTIR provides information on the functional groups and molecular bonding within materials, particularly useful in detecting chemical modifications and degradation [2].

This research aims to integrate these three complementary techniques to investigate microstructural and compositional changes in materials subjected to specific treatments or environmental exposures. By correlating morphological, structural, and chemical data, this study contributes to a deeper understanding of material behavior and guides the development of improved composites with tailored properties for advanced applications.



Figure 1: Scanning electron microscope (SEM)



Figure 2: Philips X-pert multipurpose x-ray diffractometer



Figure 3: Perkin-elmer spectrum RXI, (FTIR) spectrometer

## LITERATURE REVIEW

Microstructural characterization plays a vital role in understanding the behavior and performance of engineering materials. Over the years, several researchers have employed advanced analytical techniques to study the structural, morphological, and chemical evolution of materials under various processing and environmental conditions.

*Scanning Electron Microscopy (SEM)* has been extensively used to examine surface morphology, particle size distribution, porosity, and failure mechanisms in diverse materials such as ceramics, polymers, metals, and composites. According to Zhang et al. (2017), SEM imaging enabled the identification of voids and crack propagation in thermally treated polymer composites, revealing the correlation between microstructure and mechanical degradation. Similarly, Kumar and Singh (2020) reported significant changes in particle bonding and surface texture in fly ash-based composites using SEM micrographs.

*X-Ray Diffraction (XRD)* is a fundamental tool for identifying crystallographic phases and detecting phase transitions. It has been widely applied to analyze the crystalline structure of treated and untreated materials. In the study by Gupta and Mehta (2018), XRD was utilized to assess the degree of crystallinity in nano-reinforced composites, demonstrating a shift in diffraction peaks due to thermal exposure. Li et al. (2016) showed that XRD patterns could effectively capture the amorphous-to-crystalline transformation in geopolymer materials subjected to high-temperature curing.

*Fourier Transform Infrared Spectroscopy (FTIR)* offers complementary insights by identifying functional groups and chemical bonding within the material matrix. FTIR has been successfully used to analyze hydration products in cementitious materials (Sharma et al., 2019), detect silicate and aluminate bonding in fly ash and slag-based systems (Roy & Das, 2017), and investigate degradation in polymer chains. These studies underscore the ability of FTIR to reveal subtle chemical changes not visible through morphological techniques alone.

Combined use of SEM, XRD, and FTIR has proven to be a powerful approach for comprehensive microstructural evaluation. For instance, Patel et al. (2021) integrated all three techniques to study thermal aging effects in hybrid composites and observed consistent changes in morphology, crystalline structure, and chemical composition.

In summary, literature reveals that while each technique individually provides valuable information, their synergistic application enables a holistic understanding of microstructural changes. This reinforces the need for integrated analysis, particularly for complex or hybrid materials, which is the focus of the present study.

## EXPERIMENTAL WORK

Laboratory investigations offer a precise and controlled approach to evaluate the numerous parameters encountered in practical applications. This section provides a brief overview of the materials used, sample preparation methods, and the characterization techniques employed such as SEM, XRD, and FTIR. It also outlines the evaluation of key mechanical and surface properties, including compressive strength, hardness, wear resistance, and thermal conductivity.

### 3.1 Materials Used

#### 3.1.1 Fly Ash

The fly ash used in this project was sourced in dry form from the electrostatic precipitators of the Captive Power Plant (CPP-II). The collected fine powder was oven-dried at a temperature range of 110°C to 160°C and then stored in an airtight container for future use.

#### 3.1.2 Cold Setting Resin and Binder

The resin and hardener used in this process were supplied by SRM Marketing LLP (Limited Liability Partnership) – Ajmer. A notable manufacturer and supplier of epoxy resins and infusion systems in Ajmer.

They offer Atul Brand epoxy resins which are well-suited as cold-mounting binders due to their strong bonding, good chemical resistance, and rapid curing characteristics qualities ideal for FA resin applications. They offer: pure epoxy resin powders or liquids, Compatible hardeners/accelerators.

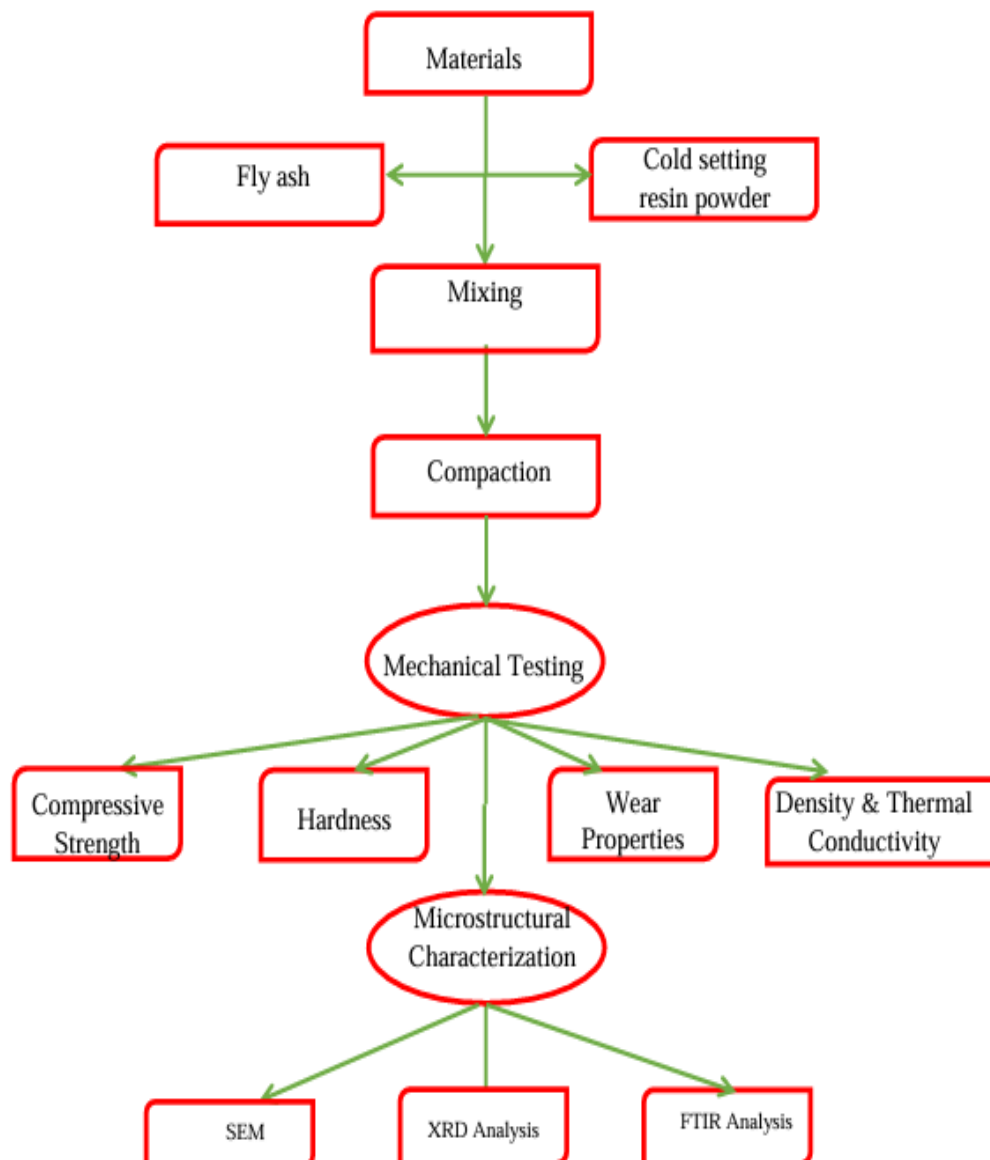


Figure 4: Flow chart of experimental procedure

## RESULTS AND DISCUSSION

### 4.1 Composition of Fly Ash

Fly ash primarily comprises Silica ( $\text{SiO}_2$ ), Alumina ( $\text{Al}_2\text{O}_3$ ), Calcium Oxide ( $\text{CaO}$ ), and Iron Oxide ( $\text{Fe}_2\text{O}_3$ ). Its detailed chemical composition is presented in Table 4.1.

**Table 4.1**  
**Chemical Composition Analysis Of Fly Ash**

Compounds	$\text{SiO}_2$	$\text{Al}_2\text{O}_3$	$\text{CaO}$	Mgo	$\text{P}_2\text{O}_5$	$\text{Fe}_2\text{O}_3$	$\text{SO}_3$	$\text{K}_2\text{O}$	LOI
Composition (%)	54.5	26.5	2.1	0.57	0.6	-	-	-	14.18

### 4.2 XRD Analysis

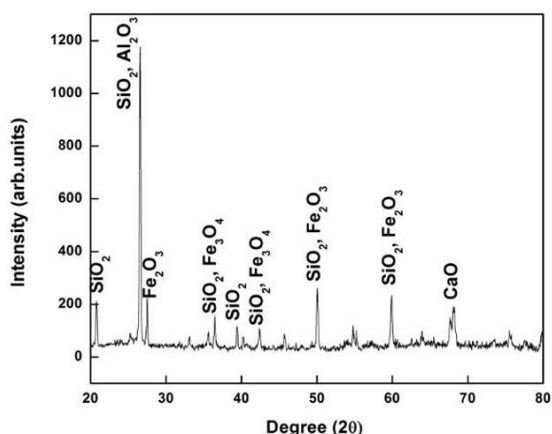


**Figure 5: (a) XRD analysis of fly ash**

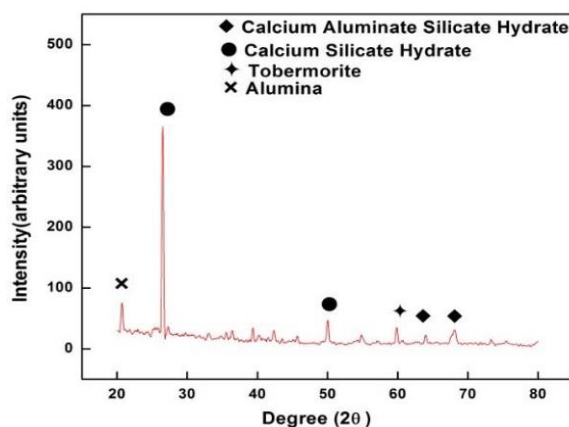


**Figure 5: (b) XRD analysis of water cured compact**

Figure 5 (a) illustrates that fly ash particles predominantly consist of silica ( $\text{SiO}_2$ ) and alumina ( $\text{Al}_2\text{O}_3$ ), which are the major reactive components responsible for the pozzolanic activity. Figure 5 (b) presents the X-ray diffraction (XRD) analysis of compacts treated with water, revealing the formation of new crystalline phases. When exposed to moisture, a pozzolanic reaction takes place wherein the reactive silica and alumina from fly ash react with calcium hydroxide [ $\text{Ca}(\text{OH})_2$ ] in the presence of water. This reaction results in the formation of calcium silicate hydrate (C–S–H) and calcium aluminate silicate hydrate (C–A–S–H) phases.

These hydration products play a critical role in the solidification and hardening of unfired fly ash compacts. They significantly enhance the inter-particle bonding, resulting in denser microstructures and improved mechanical properties such as increased hardness and strength. Over time, the initially formed C–S–H and C–A–S–H phases may undergo further transformation into a semi-crystalline compound known as Tobermorite (chemical formula:  $\text{C}_5\text{S}_6\text{H}_5$ ), which contributes further to the mechanical stability and durability of the composite material.

### 4.3 FTIR Analysis

Figure 6 displays the Fourier Transform Infrared Radiation (FTIR) spectra of pure fly ash (100% FA) and a composite mixture containing 80% fly ash and 20% resin polymer (RP). A noticeable reduction in transmittance (%) is observed in the 80% FA + 20% RP mix compared to the 100% FA sample, indicating chemical and structural changes due to the addition of resin polymer.

By comparing the FTIR spectra, phase transformations between the pure FA and the FA–RP composite are evident. One of the most prominent differences is the shifting of bands associated with the asymmetric stretching vibrations of Si–O–Si and Al–O–Si bonds. In the FTIR spectrum, a broad band observed around  $1250\text{ cm}^{-1}$  for the 100% FA sample becomes sharper in the FA–RP mix, indicating structural reorganization and polymer network formation.

Additionally, these bands shift toward lower wave numbers, settling around  $950\text{ cm}^{-1}$ , suggesting the formation of a gel-like aluminosilicate phase. This transformation is associated with the reaction of fly ash particles in a strongly alkaline environment, where active silica and alumina species dissolve and reprecipitate as a geopolymeric gel.

A distinct stretching vibration of the Si–O–Al bond appears around  $600\text{ cm}^{-1}$ , further confirming the development of a new aluminosilicate network. Furthermore, broad absorption bands observed near  $3500\text{ cm}^{-1}$  in both spectra correspond to the stretching (–OH) and bending (H–O–H) vibrations of water molecules. These vibrations are due to moisture adsorbed on the surface or trapped within the pores of the polymeric matrix. The broad nature of this band indicates the presence of strong hydrogen bonding, which is typical in geopolymer structures and supports the formation of a stable, hydrated network.

In conclusion, water content plays a critical role in influencing the mechanical strength of the synthesized composites. The FTIR spectra exhibit peaks around  $2400\text{ cm}^{-1}$ , corresponding to O–H stretching vibrations. A gradual decrease in both the intensity and broadness of this band indicates the loss of water from the system. Additionally, a broad peak observed in the  $3000\text{--}2000\text{ cm}^{-1}$  range is attributed to C–H stretching vibrations, likely arising from organic contaminants introduced during sample handling or due to residual hydrocarbons naturally present in fly ash.

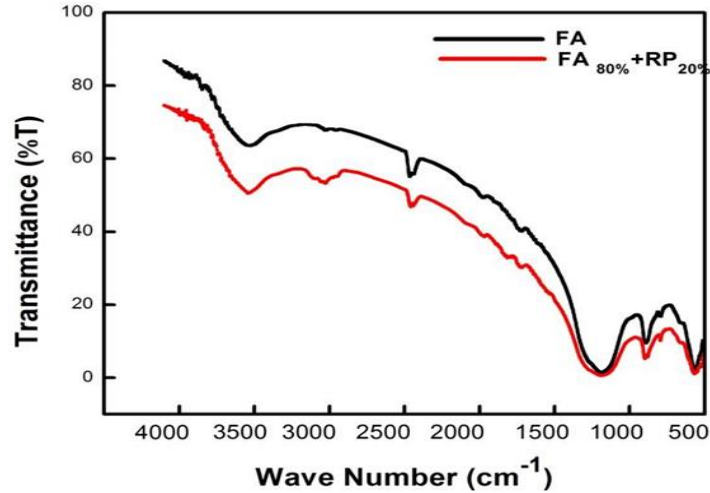


Figure 6: IR spectra of the FA and FA resin powder mix

#### 4.4 SEM Analysis

The microstructure of the composites containing 75%, 80%, and 85% by weight of fly ash (FA) mixed with resin powder was examined using Scanning Electron Microscopy (SEM) at various magnifications. The particle size of the FA powder was also analyzed and found to range between  $9.63\text{ }\mu\text{m}$  and  $47.6\text{ }\mu\text{m}$ .

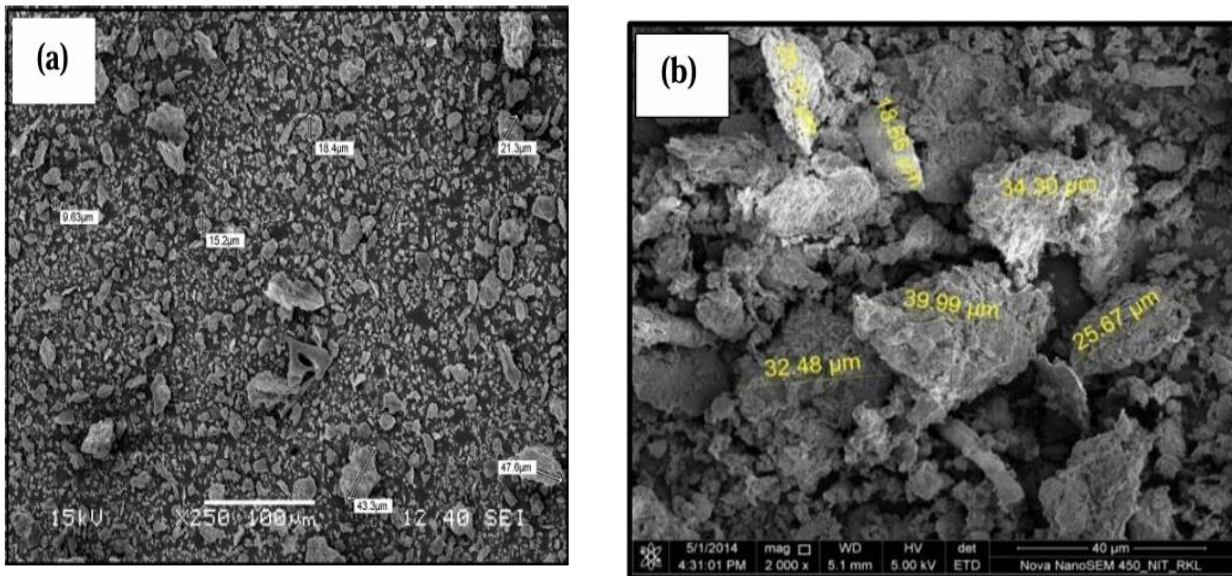


Figure 7: (a & b) Particle size distribution of FA powder at different magnification

SEM micrographs reveal that fly ash (FA) particles are predominantly spherical, irregular, and loosely agglomerated. In the case of the 75 wt.% FA composition, as shown in figure 8 (a), visible cracks appear along the inter-particle boundaries, indicating a porous interface.

As the polymer content decreases (i.e., FA content increases), the interface bonding appears to improve, resulting in fewer cracks. However, with a further reduction in resin content, although overall compaction improves, elongated cracks and cavities begin to appear along the particle boundaries.

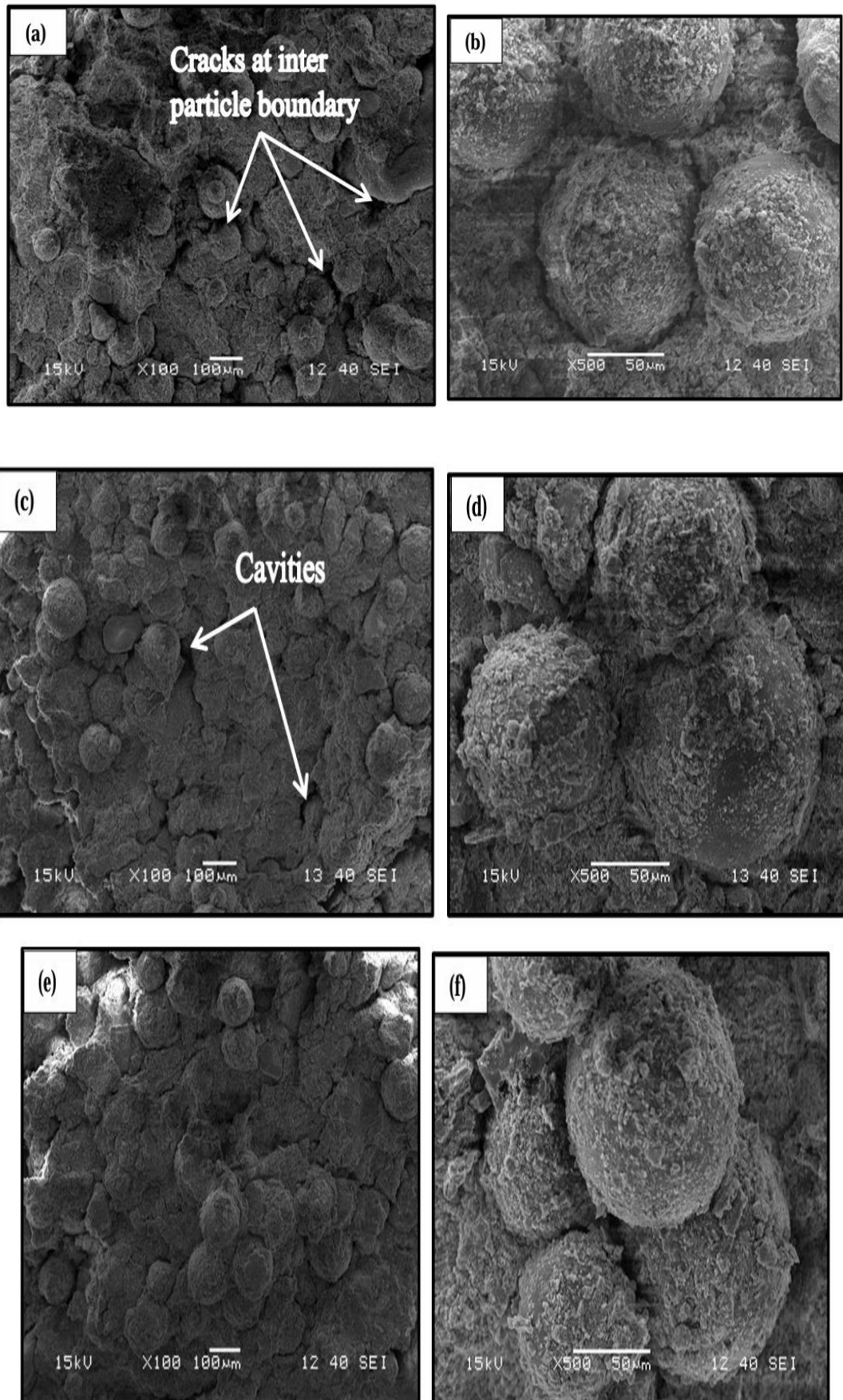


Figure 8: Morphology of Fly ash compacts with different composition and at different magnifications

Figure 9 presents the FESEM micrographs of the wear tracks along the sliding direction at various magnifications. The images indicate that the predominant wear mechanisms include delamination, surface ploughing, micro-crack formation, and tribolayer rubbing.

In figure 9 (a), micro-cracks are observed initiating perpendicular to the sliding direction, contributing to surface wear. Figure 9 (c) displays the wear track of dry compacts with 80% FA composition at a lower magnification.

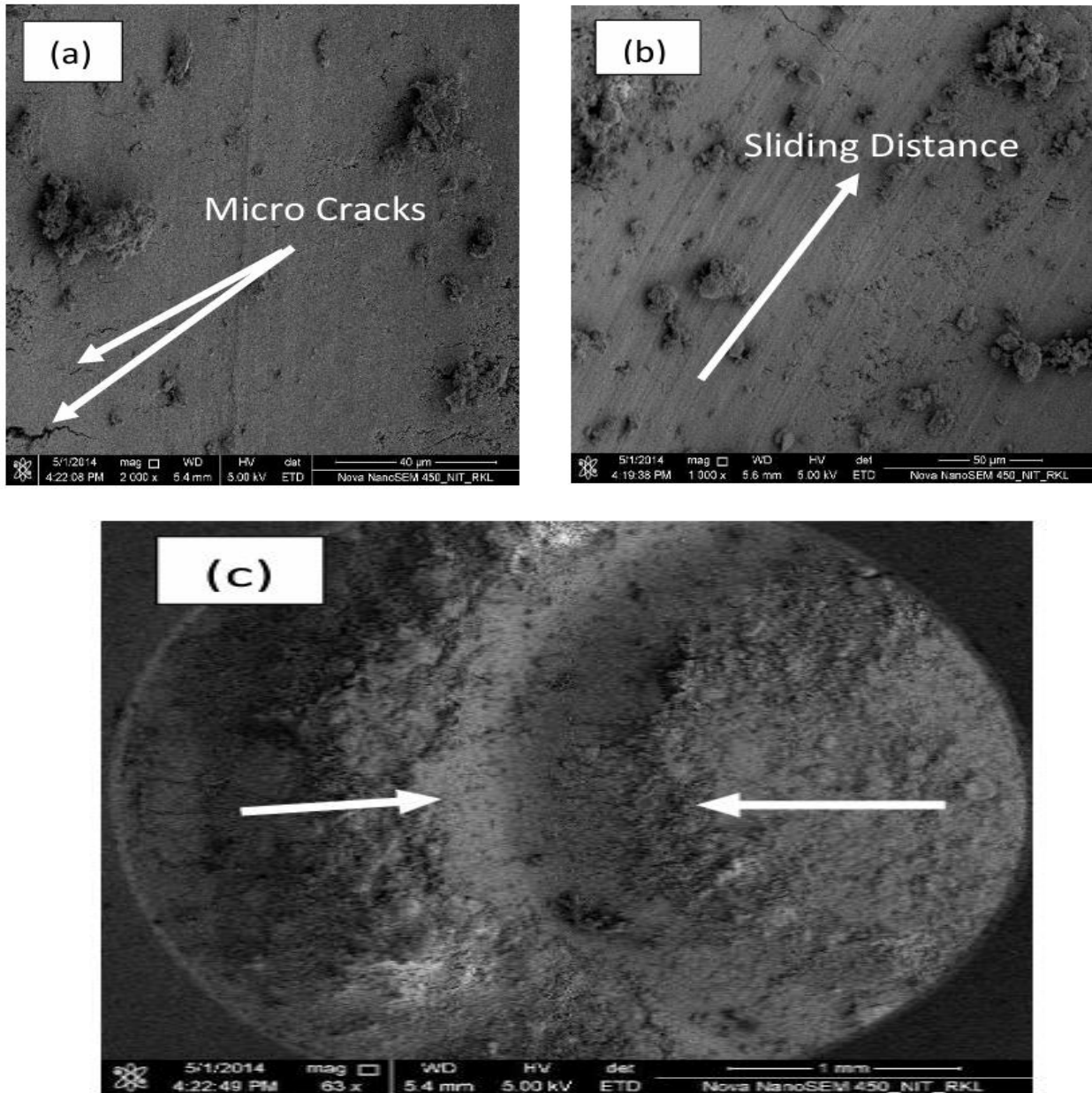


Figure 9: FESEM image of wear track at different magnification

## CONCLUSION

This study effectively demonstrates the significance of using advanced characterization techniques Scanning Electron Microscopy (SEM), X-Ray Diffraction (XRD), and Fourier Transform Infrared Spectroscopy (FTIR) to investigate the microstructural changes in fly ash-based materials. SEM analysis provided detailed insights into the surface morphology, particle distribution, and porosity variations of fly ash composites under different conditions. XRD revealed the crystalline and amorphous phase transformations, confirming the presence of essential mineralogical components such as quartz, mullite, and other aluminosilicate phases.

FTIR spectroscopy further validated chemical interactions by identifying functional groups and bonding behavior, particularly the presence of Si–O–Si and Al–O–Si linkages, which play a crucial role in the strength and stability of fly ash matrices.

The integrated approach allowed for a comprehensive understanding of the physical, structural, and chemical evolution occurring in fly ash materials due to environmental or thermal exposure. These findings not only enhance our knowledge of fly ash behavior but also contribute to the optimization of fly ash-based composites for applications in construction, waste utilization, and sustainable material development. Future studies can further explore the effect of various additives, curing conditions, and long-term durability using similar multi-technique characterization strategies.

The fly ash–resin powder composites developed in the present study demonstrate promising potential for application as sustainable construction materials. Their favorable mechanical, thermal, and wear properties suggest they can serve as viable alternatives to traditional building materials, particularly in the manufacturing of bricks and structural components. Utilizing fly ash in this manner not only adds value to what is typically considered industrial waste but also supports environmental sustainability by reducing dependency on natural clay resources.

## REFERENCES

1. P. Kumar, H. S. Gupta, M. Singh, A. S. Chaudhari, A. K. Maurya, and G. Manik, “Mechanical, thermal, and morphological analysis of Himalayan agave fiber/GO-coated fly ash hybrid polypropylene composites,” *Chemistry – A European Journal*, vol. 31, no. 2, e202402393, 2025.
2. S. S. Nordin, E. E. Mhd Noor, and P. Chockalingam, “Chemical and thermal analysis of fly ash-reinforced aluminum matrix composites (AMCs),” *Journal of Composite Science*, vol. 8, no. 5, art. 170, 2024.
3. S. Nagaraja, P. B. Anand, S. H. D., and M. I. Ammarullah, “Influence of fly ash filler on the mechanical properties and water absorption behaviour of epoxy polymer composites reinforced with pineapple leaf fibre for biomedical applications,” *RSC Advances*, vol. 14, pp. 14680–14696, 2022.
4. S. Nagendiran, A. Badghaish, I. A. Hussein, A. N. Shuaib, S. A. Furquan, and M. H. Al-Mehthel, “Epoxy/oil fly ash composites prepared through in situ polymerization: enhancement of thermal and mechanical properties,” *Polymer Composites*, vol. 37, no. 2, pp. 512–522, 2016.
5. K. Hemra, T. Kobayashi, P. Aungkavattana, and S. Jiemsirilers, “Enhanced mechanical and thermal properties of fly ash-based geopolymer composites by wollastonite reinforcement,” *Journal of Metals, Materials and Minerals*, vol. 31, no. 4, pp. 13–25, Dec. 2021.
6. N. K. A. Agustini, A. Triwiyono, D. Sulistyono, and S. Suyitno, “Mechanical properties and thermal conductivity of fly ash-based geopolymer foams with polypropylene fibers,” *Applied Sciences*, vol. 11, no. 11, art. 4886, May 2019.
7. G. Yu and Y. Jia, “Microstructure and mechanical properties of fly ash-based geopolymer cementitious composites,” *Minerals*, vol. 12, no. 7, art. 853, Jul. 2018.
8. M. H. Yazid *et al.*, “Mechanical properties of fly ash-based geopolymer concrete incorporation nylon66 fiber,” *Materials*, vol. 15, no. 24, art. 9050, Dec. 2020.
  - A. K. Ram and S. Mohanty, “State of the art review on physiochemical and engineering characteristics of fly ash and its applications,” *International Journal of Coal Science & Technology*, vol. 9, art. 9, Mar. 2022.
9. R. Kumar, P. Tomar, A. Srivastava, and R. Lakhani, “Improvement of mechanical and microstructure properties of modified fly ash-blended low carbon cement with hydroxy propyl methyl cellulose polymer,” *Iran J Sci Technol Trans Civ Eng*, vol. 46, pp. 4219–4232, Apr. 2023.